Design of a long-term memory genetic toggle switch inspired by chromatin modification circuits

Ukjin Kwon, Hsin-Ho Huang and Domitilla Del Vecchio

***Abstract*— A genetic toggle switch, a bistable gene-regulatory network, has many biotechnology applications, from environmental sensing to therapeutics. In order for a toggle switch to be practically useful, it should be able to maintain either of its states for a sufficiently long time. While a number of bistable circuit designs have appeared, it remains a challenge to control the duration of memory of the two states due to the presence of noise. To address this problem, we propose a bacterial toggle switch design that is inspired by a chromatin modification circuit ubiquitous in mammalian systems. We specifically propose a bacterial implementation based on two DNA invertases, in which each invertase is auto-catalyzing its own expression while also catalyzing the other invertase's repression. We perform a mathematical analysis of the time to memory loss of the circuit's stable states in a simplified stochastic model of the system. Our analysis shows that we can increase the time to memory loss by increasing the expression rates of the invertases, allowing to design the circuit for long-term memory. As a comparison, we also analyze two additional designs based on invertases, a published one, and a simpler version of our design. We demonstrate that for these circuits, there is no design parameter that allows to extend the time to memory loss, thereby highlighting structural properties of our design necessary for long-term memory. We validate the theoretical findings by stochastic simulations of the full set of reactions describing the circuits. More broadly, our results provide criteria for designing long-term memory toggle switches in bacteria.**

I. INTRODUCTION

Genetic toggle switches have been used for various applications in biotechnology, including the development of a genetic timer [1], the construction of a synthetic genetic clock [2], and the formation of biofilms in response to engineered stimuli [3]. In many applications, it is highly desirable that the toggle switch maintains the memory of the input stimulus for long time, such as in sensing applications in the environment or in the gut [4] [5].

A class of toggle switch designs that appeared in the literature is based on DNA invertases [6] [7]. A DNA invertase irreversibly flips the orientation of a DNA sequence and, as such, provides a potential way to trigger an irreversible state change, thereby allowing long-term memory. By using two such invertases to flip the same sequence of DNA (a promoter, for example) in two opposite directions (Fig. 1(a)) is thus possible to create a switch that can be toggled between two states. Specifically, the state can be toggled by transiently inducing the expression of one invertase or the other [6]. However, despite the irreversibility of the DNA invertase flipping, this type of design looses memory rather quickly (less than three days) due to leaky expression of the DNA invertases. Although leaky expression of the invertases can be reduced to some extent, it cannot be set to zero.

We tackle this problem by proposing a design where easily tunable circuit parameters can be adjusted in order to attenuate the effect of the leakiness on the time to memory loss. Specifically, we draw inspiration from a nucleosome modification circuit, implied in epigenetic cell memory [8]. This circuit is constituted of a set of coupled enzymatic reactions that modify nucleosomes in either of two opposing states. These two nucleosome states auto-catalyze and also cross-catalyze the de-modification of the opposing state. All modifications are subject to some basal (leaky) rate. This circuit structure has been shown to lead to a bistable system and to long-term memory despite leakiness and noise since the effect of leakiness can be minimized when the auto and cross catalysis reaction rates become large compared to leakiness [9]. Given that the process by which DNA invertases flip a DNA sequence can be well captured by an enzymatic reaction, we propose to realize this enzymatic circuit motif by means of two DNA invertases as shown in Fig. 1(b). To better shed light on the core mechanism by which long-term memory is achievable, we also analyze a simpler design, which removes one of the DNA states (Fig. 1(c)).

In all cases, we start the analysis with the full set of reactions, we then write the corresponding ordinary differential equation (ODE) models, for which we perform both stability analysis and model order reduction using time scale separation. Specifically, in all cases, we reduce the model to a generalized birth and death process, whose corresponding Markov chain can be analytically solved for the time to memory loss. In all designs the time to memory loss decreases with leakiness. In our new design only, the time to memory loss can be arbitrarily increased by increasing the production rates of the DNA invertases. We then validate the analytically predicted trends by performing stochastic simulations of the original full set of reactions.

The remainder of this paper is organized as follows: Section II describes the construction of toggle switch in [6] and our toggle switches. Section III provides mathematical analyses of the toggle switch designs using deterministic models. Section IV provides mathematical analysis of the time to memory loss using a stochastic model. The results from Section IV are supported by numerical simulations in

This work was supported by KFAS and AFOSR grant FA9550-14-1-0060.
U. Kwon is with the EECS Department, MIT, Cambridge, MA, H. Huang is with the Mechanical Engineering Department, MIT, Cambridge, MA and D. Del Vecchio is with the Mechanical Engineering Department, MIT, Cambridge, MA. Emails: ujkwon@mit.edu, hh_huang@mit.edu and ddv@mit.edu

Section V. Finally, Section VI concludes the paper.

II. Construction of a toggle switch using a pair of DNA invertases

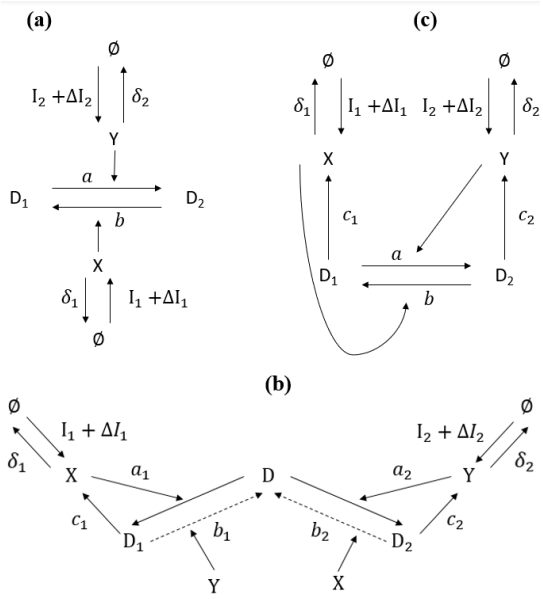

Fig. 1: **Diagrams of toggle switch designs.** (a) Diagram of the circuit in [6]. The D_1 state can be flipped to the D_2 state by a DNA invertase Y and the D_2 state can be flipped back to the D_1 state by another DNA invertase X. X and Y can be produced by an inducible expression system with production rate constant I_1 and I_2, respectively, and it can be diluted with dilution rate constants δ_1 and δ_2, respectively. There is a basal level expression of X and Y with rate ΔI_1 and ΔI_2, respectively. (b) Three-state auto-catalytic design. The baseline DNA D state can be flipped to the D_1 state and D_2 state by the DNA invertase X and Y, respectively. D_1 and D_2 can be flipped back to D by another DNA invertase Y and X, respectively. X and Y can be expressed in the D_1 state and the D_2 state, respectively (two autocatalytic structures). (c) Two-state auto-catalytic design (simplified version of (b) by removing the intermediate stated D). The D_2 state can be flipped to the D_1 state by the DNA invertase X, and X can be expressed in the D_1 state (the first autocatalytic structure). Also, the D_1 state can be flipped to the D_2 state by the other DNA invertase Y, and Y can be expressed in the D_2 state (the second autocatalytic structure).

A pair of complementary irreversible DNA invertases, FimE and HbiF, operates as follows [6] [10]. When one invertase flips the DNA, it constructs the recognition site for the other and viceversa. To be more specific, FimE recognizes the DNA sequence (A_1, A_2) and (B_2, B_1), where A_1, A_2, B_1, B_2 are given DNA sequences, and flips the entire DNA sequence from A_2 to B_2. Then HbiF recognizes the DNA sequence $(A_1, \bar{B_2})$ and $(\bar{A_2}, B_1)$, where $\bar{B_2}$ is the flipped B_2 sequence, and $\bar{A_2}$ is the flipped A_2 sequence, which results in HbiF flippling back the entire DNA sequence from $\bar{B_2}$ to $\bar{A_2}$ [6].

In [6], the authors built a toggle switch with FimE and HbiF, which can be represented by the diagram in Fig. 1(a). From the D_1 state, HbiF (Y) can recognize the sequence $(A_1, \bar{B_2})$ and $(\bar{A_2}, B_1)$ and flip the entire DNA sequence from $\bar{B_2}$ to $\bar{A_2}$, and the D_1 state is flipped to the D_2 state. From the D_2 state, FimE (X) can recognize the sequence (A_1, A_2) and (B_2, B_1) and flip the entire DNA sequence from A_2 to B_2 and the D_2 state is flipped to the D_1 state. To flip the state from D_1 to D_2, or viceversa, Y or X must be overexpressed from its corresponding inducible promoter, represented here by a production rate I. Here, ΔI represents the leakiness of expression of the inducible promoters. In [6], it was shown that this toggle switch loses its memory in 2 days because both invertases are continuously expressed due to basal expression, even it is not intended.

To overcome this issue, we propose a toggle switch design inspired by chromatin modification circuits [9] and use the same DNA invertases, as above (Fig. 1(b)). In this design, FimE (X) can recognize the sequence (A_1, A_2) and (B_2, B_1) present in the D state and flips it to the D_1 state. From the D_1 state in turn, FimE is expressed, thereby creating an autocatalytic loop. Then, from the D_1 state, HbiF can recognize the sequence $(A_1, \bar{B_2})$ and $(\bar{A_2}, B_1)$, and flips it back to the baseline DNA D state. Also, from the D state, HbiF can recognize the sequence $(A_1, \bar{B_2})$ and $(\bar{A_2}, B_1)$, and flips it to the D_2 state. From the D_2 state, HbiF (Y) can be expressed, thereby creating a second autocatalytic loop. Then, from the D_2 state, FimE in turn, can recognize the sequence (A_1, A_2) and (B_2, B_1), and flips it back to the D state. In addition, to externally trigger a state change, X and Y are each expressed by inducible promoters as in the previous design. In order to better determine the critical circuit's requirement for long-term memory, we also analyze a simplified design, in which the baseline DNA state D is not present (Fig. 1(c)). In the next section, we introduce the mathematical models of these systems for subsequent analysis.

III. Stability analysis of the toggle switch designs and model reduction

A. Mathematical model of the design in Fig. 1(a)

This is a design that was proposed in [6] as a way to keep persistent expression of either one of two possible gene expression states. Based on Fig. 1(a), the reactions can be written as

$$\begin{aligned} &D_1 + Y \xrightarrow{a} D_2 + Y, \quad D_2 + X \xrightarrow{b} D_1 + X, \\ &X \underset{I_1+\Delta I_1}{\overset{\delta_1}{\rightleftharpoons}} \emptyset, \quad Y \underset{I_2+\Delta I_2}{\overset{\delta_2}{\rightleftharpoons}} \emptyset, \end{aligned} \tag{1}$$

where, D_1 is the first state, D_2 is the second state, X is the first invertase that flips D_2 to D_1 with flipping rate constant b, Y is the second invertase that flips D_1 to D_2 with flipping rate constant a. Here, δ_1 and δ_2 are dilution rate constants of X and Y, respectively, I_1 and I_2 are production rate constants of X and Y due to external induction of the invertases, respectively, and ΔI_1 and ΔI_2 are basal expression rate

constants of X and Y, respectively, or leakiness, which in an ideal system should be exactly zero. In practice, however, the genes that are expressing X and Y, even if inducible, will always have a low level of expression. Therefore, we analyze how non-zero leakiness affects the stability properties of the system.

From (1), we can write the ODEs for the system as

$$\begin{aligned} &\frac{d}{dt}D_1 = -aD_1Y + bD_2X, \quad \frac{d}{dt}D_2 = -bD_2X + aD_1Y, \\ &\frac{d}{dt}X = (I_1 + \Delta I_1) - \delta_1 X, \quad \frac{d}{dt}Y = (I_2 + \Delta I_2) - \delta_2 Y. \end{aligned} \tag{2}$$

According to [6], the protein decay rates are much larger than the flipping rates. Therefore, the dynamics of X and Y can be regarded as the fast dynamics of system (2) and we can employ the quasi-steady state approximation [11], letting $\frac{d}{dt}X = \frac{d}{dt}Y = 0$. Therefore, without input ($I_1 = I_2 = 0$), X and Y can be approximated as $X = \frac{\Delta I_1}{\delta_1}$, $Y = \frac{\Delta I_2}{\delta_2}$, respectively, and we obtain the reduced system as follows:

$$\begin{aligned} &\frac{d}{dt}D_1 = -aD_1\frac{\Delta I_2}{\delta_2} + bD_2\frac{\Delta I_1}{\delta_1}, \\ &\frac{d}{dt}D_2 = -bD_2\frac{\Delta I_1}{\delta_1} + aD_1\frac{\Delta I_2}{\delta_2}. \end{aligned} \tag{3}$$

From (3), we observe that if the leakiness is zero ($\Delta I_1 = \Delta I_2 = 0$), then any value of (D_1, D_2) is a (marginally) stable steady state. When instead leakiness is non-zero, but very small, starting from any initial state, and in particular from $D_1 = D_{tot}$ or $D_2 = D_{tot}$, the system will very slowly approach the unique stable equilibrium $(D_1, D_2) = (\frac{b\delta_2\Delta I_1}{a\delta_1\Delta I_2 + b\delta_2\Delta I_1}D_{tot}, \frac{a\delta_1\Delta I_2}{a\delta_1\Delta I_2 + b\delta_2\Delta I_1}D_{tot})$. This shows that, under the realistic scenario where we have leakiness, the system will always have a unique intermediate stable equilibrium and will not be bistable. Therefore, this system is not a good candidate for achieving persistent expression of more than one gene expression states. Nevertheless, since this was proposed in the literature as a potential design to keep in memory an initial state given by $D_1 = 0$ or $D_1 = D_{tot}$, we will ask the question of how long the system, when initialized at either one of the two configurations $D_1 = D_{tot}$ or $D_2 = D_{tot}$, will keep this state in a stochastic model. Specifically, system (3) corresponds to the reactions given by:

$$D_1 \underset{b\frac{\Delta I_1}{\delta_1}}{\overset{a\frac{\Delta I_2}{\delta_2}}{\rightleftharpoons}} D_2, \tag{4}$$

with conservation law $D_1 + D_2 = D_{tot}$, we will use (4) to determine the hitting time of $D_1 = \frac{b\delta_2\Delta I_1}{a\delta_1\Delta I_2 + b\delta_2\Delta I_1}D_{tot}$, which is the unique stable equilibrium, starting from $D_1 = D_{tot}$, using a one-dimensional Markov chain model. This is explained in Section IV-*C*.

B. Mathematical model of the design in Fig. 1(b)

Based on Fig. 1(b), the reactions describing the system can be written as

$$\begin{aligned} &D + X \xrightarrow{a_1} D_1 + X, \quad D + Y \xrightarrow{a_2} D_2 + Y, \\ &D_1 \xrightarrow{c_1} D_1 + X, \quad D_2 \xrightarrow{c_2} D_2 + Y, \\ &D_1 + Y \xrightarrow{b_1} D + Y, \quad D_2 + X \xrightarrow{b_2} D + X, \\ &X \underset{I_1+\Delta I_1}{\overset{\delta_1}{\rightleftharpoons}} \emptyset, \quad Y \underset{I_2+\Delta I_2}{\overset{\delta_2}{\rightleftharpoons}} \emptyset, \end{aligned} \tag{5}$$

where, D is an intermediate DNA state that does not express proteins, D_1 is the first state, D_2 is the second state, X is the first invertase that flips D to D_1 and D_2 to D with flipping rate constants a_1 and b_2, respectively, Y is the second invertase that flips D to D_2 and D_1 to D with flipping rate constants a_2 and b_1, respectively. Parameters c_1 and c_2 are expression rate constants of X and Y from D_1 and D_2, respectively. Parameters δ_1 and δ_2 are dilution rate constants of X and Y, respectively, I_1 and I_2 are production rate constants of X and Y due to external induction of the invertases, respectively, and ΔI_1 and ΔI_2 are basal expression rate constants of X and Y, respectively.

From (5), we can write the ODEs of our system as

$$\begin{aligned} &\frac{d}{dt}D = -a_1DX - a_2DY + b_1D_1Y + b_2D_2X, \\ &\frac{d}{dt}D_1 = a_1DX - b_1D_1Y, \quad \frac{d}{dt}D_2 = a_2DY - b_2D_2X, \\ &\frac{d}{dt}X = c_1D_1 - \delta_1X + I_1 + \Delta I_1, \\ &\frac{d}{dt}Y = c_2D_2 - \delta_2Y + I_2 + \Delta I_2. \end{aligned} \tag{6}$$

According to [6] and [12], protein decay rates are much larger than the flipping rates, so the dynamics of X and Y can be approximated at the quasi-steady state. Therefore, without input ($I_1 = I_2 = 0$), X and Y can be approximated as $X = \frac{c_1D_1 + \Delta I_1}{\delta_1}$ and $Y = \frac{c_2D_2 + \Delta I_2}{\delta_2}$, respectively. Also, according to [9], if a_1 and a_2 are sufficiently larger than b_1 and b_2, D can be regarded as a fast variable and it can be approximated as $D = \frac{b_1D_1Y + b_2D_2X}{a_1X + a_2Y}$. Here, we use this approximation to perform an analytical investigation of (6). We then validate the analytical findings against stochastic simulations of the original system of reactions (5) that does not have this time scale separation to show that our analytical finding is still predictive of the trends (Section V).

We thus obtain the reduced model as follows:

$$\begin{aligned} &\frac{d}{dt}D_1 = -\frac{a_2b_1Y^2}{a_1X + a_2Y}D_1 + \frac{a_1b_2X^2}{a_1X + a_2Y}D_2, \\ &\frac{d}{dt}D_2 = \frac{a_2b_1Y^2}{a_1X + a_2Y}D_1 - \frac{a_1b_2X^2}{a_1X + a_2Y}D_2. \end{aligned} \tag{7}$$

From (7), we observe that if the leakiness is zero, then $(D_1, D_2) = (D_{tot}, 0)$ and $(0, D_{tot})$ are stable steady states while $(0, 0)$ and $(\frac{\frac{a_2b_1c_2^2\delta_1^2}{a_1b_2c_1^2\delta_2^2}}{1 + \frac{b_1c_2\delta_1}{a_1c_1\delta_2} + \frac{a_2b_1c_2^2\delta_1^2}{a_1b_2c_1^2\delta_2^2}}D_{tot}, \frac{1}{1 + \frac{b_1c_2\delta_1}{a_1c_1\delta_2} + \frac{a_2b_1c_2^2\delta_1^2}{a_1b_2c_1^2\delta_2^2}}D_{tot})$ are unstable steady states. When leakiness is non-zero, but $\frac{\Delta I}{c}$ is very small, the system still maintains bistability with two stable steady states approximately given by $D_1 \approx D_{tot}$ and

$D_2 \approx D_{tot}$. Therefore, we will ask the question of how long the system, when initialized at either one of the two stable configurations ($D_1 = D_{tot}$ or $D_2 = D_{tot}$), will keep this state in a stochastic model. System (7) corresponds to the reactions given by:

$$D_1 \underset{\frac{a_1 b_2 X^2}{a_1 X + a_2 Y}}{\overset{\frac{a_2 b_1 Y^2}{a_1 X + a_2 Y}}{\rightleftharpoons}} D_2, \tag{8}$$

where $X = \frac{c_1 D_1 + \Delta I_1}{\delta_1}$ and $Y = \frac{c_2 D_2 + \Delta I_2}{\delta_2}$, with a conservation law $D_1 + D_2 = D_{tot}$. We will thus use (8) to analytically determine the hitting time of $D_1 = 0$ starting from $D_1 = D_{tot}$, using a one-dimensional Markov chain model. This is explained in Section IV-*A*.

C. Mathematical model of the design in Fig. 1(c)

Based on Fig. 1(c), the reactions describing the system can be written as

$$\begin{aligned} &D_1 + Y \xrightarrow{a} D_2 + Y, \quad D_2 + X \xrightarrow{b} D_1 + X, \\ &D_1 \xrightarrow{c_1} D_1 + X, \quad D_2 \xrightarrow{c_2} D_2 + Y, \\ &X \underset{I_1 + \Delta I_1}{\overset{\delta_1}{\rightleftharpoons}} \emptyset, \quad Y \underset{I_2 + \Delta I_2}{\overset{\delta_2}{\rightleftharpoons}} \emptyset, \end{aligned} \tag{9}$$

where, D_1 is the first state, D_2 is the second state, X is the first invertase that flips D_2 to D_1 with flipping rate constant b, Y is the second invertase that flips D_1 to D_2 with flipping rate constant a. Here, c_1 and c_2 are expression rate constants of X and Y from D_1 and D_2, respectively. Parameters δ_1 and δ_2 are dilution rate constants of X and Y, respectively, I_1 and I_2 are production rate constants of X and Y due to external induction of the invertases, respectively, and ΔI_1 and ΔI_2 are basal expression rate constants of X and Y, respectively.

From (9), we can write the ODEs of our model as

$$\begin{aligned} &\frac{d}{dt} D_1 = -aD_1 Y + bD_2 X, \quad \frac{d}{dt} D_2 = aD_1 Y - bD_2 X, \\ &\frac{d}{dt} X = c_1 D_1 - \delta_1 X + I_1 + \Delta I_1, \\ &\frac{d}{dt} Y = c_2 D_2 - \delta_2 Y + I_2 + \Delta I_2. \end{aligned} \tag{10}$$

As before, the dynamics of X and Y can be approximated at the quasi-steady state. Without input ($I_1 = I_2 = 0$), X and Y can thus be approximated as $X = \frac{c_1 D_1 + \Delta I_1}{\delta_1}$, $Y = \frac{c_2 D_2 + \Delta I_2}{\delta_2}$, respectively, and we can obtain the reduced ODE model as follows:

$$\begin{aligned} \frac{d}{dt} D_1 &= -aD_1 \frac{c_2 D_2 + \Delta I_2}{\delta_2} + bD_2 \frac{c_1 D_1 + \Delta I_1}{\delta_1}, \\ \frac{d}{dt} D_2 &= aD_1 \frac{c_2 D_2 + \Delta I_2}{\delta_2} - bD_2 \frac{c_1 D_1 + \Delta I_1}{\delta_1}. \end{aligned} \tag{11}$$

From (11), we observe that if the leakiness is zero ($\Delta I_1 = \Delta I_2 = 0$), then $(D_1, D_2) = (D_{tot}, 0)$ and $(0, D_{tot})$ are stable steady states. When leakiness is non-zero, but $\frac{\Delta I}{c}$ is very small, the system still maintains bistability with two stable steady states given by $D_1 \approx D_{tot}$ and $D_2 \approx D_{tot}$. We will therefore ask the question of how long the system, when initialized at either one of the two configurations $D_1 = D_{tot}$ or $D_2 = D_{tot}$, will keep this state in a stochastic model. Specifically, system (11) corresponds to the reactions given by:

$$D_1 \underset{b\frac{c_1 D_1 + \Delta I_1}{\delta_1}}{\overset{a\frac{c_2 D_2 + \Delta I_2}{\delta_2}}{\rightleftharpoons}} D_2, \tag{12}$$

with conservation law $D_1 + D_2 = D_{tot}$. We will thus use (12) to determine the hitting time of $D_1 = 0$ starting from $D_1 = D_{tot}$, using a one-dimensional Markov chain model. This is explained in Section IV-*B*.

IV. Mathematical analysis of the time to memory loss using a stochastic model

While in a deterministic model, a bistable system initialized at a stable steady state will remain at this state indefinitely, this is not the case in a stochastic model. In fact, the noise intrinsic in the reactions will perturb the system state even when starting at a deterministically stable equilibrium. If the resulting state perturbation is large, the system's state may reach the other stable steady state and remain in its vicinity for some time. In this case, we will say that the system has lost the memory of its initial state. Here, we mathematically quantify the time it takes to loose the memory, which we call the time to memory loss, by computing a suitable hitting time in the corresponding Markov chain model.

According to reactions (4), (8) and (12), the toggle switch dynamics can be represented by a one-dimensional Markov chain, in which the state X represents the total number of D_1 and can vary between 0 and D_{tot} (Fig. 2). For the design in Fig. 1(b) and Fig. 1(c), we are interested in determining the average time it takes to the state to reach the configuration $D_1 = 0$ starting from $D_1 = D_{tot}$. On the other hand, for the design in Fig. 1(a), we are interested in determining the average time it takes to the state to reach the $D_1 = \frac{b\delta_2 \Delta I_1}{a\delta_1 \Delta I_2 + b\delta_2 \Delta I_1} D_{tot}$, which is the unique stable equilibrium, starting from $D_1 = D_{tot}$. These times are what we take as a measure of the time to memory loss of the initial state. We compute the hitting time of $D_1 = 0$ starting from $D_1 = D_{tot}$ for systems Fig. 1(b) and Fig. 1(c), and for system Fig. 1(a), we compute the hitting time of

Markov chain representation of toggle switch models

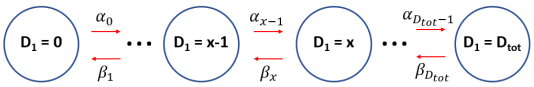

	Fig. 1(a)	Fig. 1(b)	Fig. 1(c)
α_x	$b\frac{\Delta I_1}{\delta_1}$	$\frac{a_1 b_2 (\frac{c_1 x + \Delta I_1}{\delta})^2}{a_1 \frac{c_1 x + \Delta I_1}{\delta} + a_2 \frac{c_2 (D_{tot} - x) + \Delta I_2}{\delta}}$	$b\frac{c_1 x + \Delta I_1}{\delta_1}$
β_x	$a\frac{\Delta I_2}{\delta_2}$	$\frac{a_2 b_1 (\frac{c_2 (D_{tot} - x) + \Delta I_2}{\delta})^2}{a_1 \frac{c_1 x + \Delta I_1}{\delta} + a_2 \frac{c_2 (D_{tot} - x) + \Delta I_2}{\delta}}$	$a\frac{c_2 (D_{tot} - x) + \Delta I_2}{\delta_1}$

Fig. 2: **One-dimensional Markov chain model of the toggle switch designs.** Reactions $D_1 \underset{\alpha_x}{\overset{\beta_x}{\rightleftharpoons}} D_2$ with conservation law $D_1 + D_2 = D_{tot}$ can be represented as the above Markov chain. Here, α_x and β_x of the designs in Fig. 1 are given.

$D_1 = \frac{b\delta_2\Delta I_1}{a\delta_1\Delta I_2 + b\delta_2\Delta I_1} D_{tot}$ starting from $D_1 = D_{tot}$.

A. Hitting time for the designs of Fig. 1(b) and Fig. 1(c)

We define the random variable, t_i:

$$t_i = \inf\{t \geq 0 : D_1(t) = 0; D_1(0) = i\} \text{ with } i \in [0, D_{tot}],$$

and the hitting time τ_i of $D_1 = 0$, starting from $D_1 = i$, as $\tau_i = \mathbb{E}(t_i)$. We want to calculate $\tau_{D_{tot}}$, which is the hitting time of state $D_1 = 0$, starting from state $D_1 = D_{tot}$. Then, according to [13], we have

$$\begin{aligned} &\tau_0 = 0, \\ &\tau_x = \frac{1}{\alpha_x + \beta_x} + \frac{\beta_x}{\alpha_x + \beta_x}\tau_{x-1} + \frac{\alpha_x}{\alpha_x + \beta_x}\tau_{x+1} \\ &(\text{for } x = 1, 2, \ldots, D_{tot} - 1), \\ &\tau_{D_{tot}} = \frac{1}{\beta_{D_{tot}}} + \tau_{D_{tot}-1}, \end{aligned} \tag{13}$$

where α_x and β_x are given in Fig. 2 for each of the designs. Define $\Delta\tau_x = \tau_{x+1} - \tau_x$ and multiply by $(\alpha_x + \beta_x)$ both sides, then we can rewrite (13) as follows:

$$\Delta\tau_{x-1} = \frac{1}{\beta_x} + \frac{\alpha_x}{\beta_x}\Delta\tau_x,$$

where $\Delta\tau_{D_{tot}-1}$ is $\tau_{D_{tot}} - \tau_{D_{tot}-1} = \frac{1}{\beta_{D_{tot}}}$. Then, we rewrite $\Delta\tau_{x-1}$ as follows:

$$\begin{aligned} &\Delta\tau_{x-1} = \frac{1}{\beta_x} + \frac{\alpha_x}{\beta_x}\Delta\tau_x = \frac{1}{\beta_x} + \frac{\alpha_x}{\beta_x}\left(\frac{1}{\beta_{x+1}} + \frac{\alpha_{x+1}}{\beta_{x+1}}\Delta\tau_{x+1}\right) \\ &= \frac{1}{\beta_x} + \frac{1}{\beta_{x+1}}\frac{\alpha_x}{\beta_x} \ldots + \frac{1}{\beta_{D_{tot}-1}}\frac{\alpha_x\alpha_{x+1}\ldots\alpha_{D_{tot}-2}}{\beta_x\beta_{x+1}\ldots\beta_{D_{tot}-2}} \\ &+ \frac{\alpha_x\alpha_{x+1}\ldots\alpha_{D_{tot}-1}}{\beta_x\beta_{x+1}\ldots\beta_{D_{tot}-1}}\Delta\tau_{D_{tot}-1}, \end{aligned}$$

and rewrite $\Delta\tau_x$ as follows:

$$\Delta\tau_x = \sum_{j=x}^{D_{tot}-1} \frac{1}{\beta_j}\frac{\gamma_j}{\gamma_x} + \frac{\Delta\tau_{D_{tot}-1}}{\gamma_x} = \sum_{j=x}^{D_{tot}-1} \frac{1}{\beta_j}\frac{\gamma_j}{\gamma_x} + \frac{1}{\beta_{D_{tot}}\gamma_x},$$

where $\gamma_x = \frac{\beta_x\alpha_{x+1}\ldots\beta_{D_{tot}-1}}{\alpha_x\alpha_{x+1}\ldots\alpha_{D_{tot}-1}}$. We thus obtain

$$\begin{aligned} &\tau_{D_{tot}} = \tau_{D_{tot}-1} + \frac{1}{\beta_{D_{tot}}} \\ &= (\tau_{D_{tot}-1} - \tau_{D_{tot}-2}) + \ldots + (\tau_1 - \tau_0) + \frac{1}{\beta_{D_{tot}}} \\ &= \sum_{x=0}^{D_{tot}-2}\left(\sum_{j=x}^{D_{tot}-1} \frac{1}{\beta_j}\frac{\gamma_j}{\gamma_x} + \frac{1}{\beta_{D_{tot}}\gamma_x}\right) + \frac{1}{\beta_{D_{tot}}} \\ &= \frac{1}{\beta_{D_{tot}}}\left(1 + \frac{1}{\gamma_1} + \ldots + \frac{1}{\gamma_{D_{tot}-1}}\right) + \ldots \\ &+ \frac{1}{\beta_x}\left(1 + \frac{\gamma_x}{\gamma_{x-1}} + \ldots + \frac{\gamma_x}{\gamma_1}\right) + \ldots + \frac{1}{\beta_0}. \end{aligned} \tag{14}$$

We next evaluate the expression of $\tau_{D_{tot}}$ given in (14) by substituting the expression of γ_x using the expressions of α_x and β_x given in Fig. 2 for each of the designs.

Claim 4.1: Under the symmetry assumption, where $a_1 = a_2 = a$, $b_1 = b_2 = b$, $a = b$, $c_1 = c_2 = c$, $\delta_1 = \delta_2 = \delta$, $I_1 = I_2 = I$ and $\Delta I_1 = \Delta I_2 = \Delta I$, the hitting time $\tau_{D_{tot}}$ satisfies $\tau_{D_{tot}} > \frac{(D_{tot})^2}{a}\frac{\delta c}{(\Delta I)^2}$ for system Fig. 1(b)

Proof: From (14), $\tau_{D_{tot}}$ is larger than $\frac{1}{\beta_{D_{tot}}}(1 + \frac{1}{\gamma_1} + \ldots + \frac{1}{\gamma_{D_{tot}-1}})$. With the symmetry assumption,

$$\alpha_x = \beta_{D_{tot}-x} = \frac{a(\frac{cx+\Delta I}{\delta})^2}{\frac{cD_{tot}+2\Delta I}{\delta}} \text{ and } \alpha_1 < \alpha_2 < \alpha_3 \ldots < \alpha_{D_{tot}}.$$

Therefore,

$$\frac{1}{\gamma_x} = \frac{\alpha_x\alpha_{x+1}\ldots\alpha_{D_{tot}-1}}{\beta_x\beta_{x+1}\ldots\beta_{D_{tot}-1}} = \frac{\alpha_x\alpha_{x+1}\ldots\alpha_{D_{tot}-1}}{\alpha_{D_{tot}-x}\alpha_{D_{tot}-x-1}\ldots\alpha_1} \geq 1.$$

This implies,

$$\tau_{D_{tot}} \geq \frac{1}{\beta_{D_{tot}}}\left(1 + \frac{1}{\gamma_1} + \ldots + \frac{1}{\gamma_{D_{tot}-1}}\right) \geq \frac{D_{tot}}{\beta_{D_{tot}}}. \tag{15}$$

Also, by the definition of β_x given in Fig. 2, we have

$$\frac{1}{\beta_{D_{tot}}} = \frac{\frac{acD_{tot}}{\delta} + \frac{2a\Delta I}{\delta}}{a^2(\frac{\Delta I}{\delta})^2} \geq \frac{\frac{acD_{tot}}{\delta}}{a^2(\frac{\Delta I}{\delta})^2}. \tag{16}$$

By combining (15) and (16),

$$\tau_{D_{tot}} \geq \frac{(D_{tot})^2}{a}\frac{\delta c}{(\Delta I)^2}.$$

■

We note that in this design we can increase the hitting time by increasing the value of the expression rate constant c_i of the invertases. This can be easily accomplished experimentally by increasing the strength of the ribosome binding site (RBS) or of the corresponding promoters. Therefore, we can tune the hitting time and thus, in principle, we can increase the time to memory loss of both extremal states.

Claim 4.2: Under the symmetry assumption, where $a = b$, $c_1 = c_2 = c$, $\delta_1 = \delta_2 = \delta$, $I_1 = I_2 = I$ and $\Delta I_1 = \Delta I_2 = \Delta I$, the hitting time $\tau_{D_{tot}}$ satisfies $\tau_{D_{tot}} > \frac{\delta}{a\Delta I}2^{D_{tot}-2}$ for system Fig. 1(c)

Proof: From (14), $\tau_{D_{tot}}$ is larger than $\frac{1}{\beta_{D_{tot}}}(1 + \frac{1}{\gamma_1} + \ldots + \frac{1}{\gamma_{D_{tot}-1}})$. With the symmetry assumption,

$$\begin{aligned} &\tau_{D_{tot}} > \frac{1}{\beta_{D_{tot}}}\left(1 + \frac{1}{\gamma_0} + \ldots + \frac{1}{\gamma_{D_{tot}-2}}\right) \\ &= \frac{\delta}{a\Delta I}\left(1 + \frac{c(D_{tot}-1) + \Delta I}{c + \Delta I} + \ldots\right. \\ &\left. + a\frac{(c(D_{tot}-1+\Delta I))(c(D_{tot}-2)+\Delta I)\ldots(2c+\Delta I)}{(c+\Delta I)(2c+\Delta I)\ldots((D_{tot}-1)c+\Delta I)}\right) \\ &> \frac{\delta}{2a\Delta I}\left(1 + (D_{tot}-1) + \ldots + \frac{(D_{tot}-1)(D_{tot}-2)\ldots 2}{2\times 3\times\ldots(D_{tot}-1)}\right) \\ &= \frac{\delta}{a\Delta I}2^{D_{tot}-2}. \end{aligned}$$

■

This result shows that the easily tunable parameter c_i cannot be used to extend the time to memory loss in this design and that this time is only dependent on the leakiness, on the decay rate of the proteins, mostly due to cell dilution, and to the recombinase switching rate constant, which are not as easily tunable.

B. Hitting time for the design of Fig. 1(a)

When we assume symmetry, where $a = b$, $\delta_1 = \delta_2 = \delta$, $\Delta I_1 = \Delta I_2 = \Delta I$, $\frac{b\delta_2\Delta I_1}{a\delta_1\Delta I_2 + b\delta_2\Delta I_1} D_{tot}$ becomes $\frac{1}{2}D_{tot}$. For simplicity, we consider the hitting time of $D_1 = \frac{1}{2}D_{tot}$ starting from $D_1 = D_{tot}$. We define the random variable, t_i:

$$t_i = \inf\{t \geq 0 : D_1(t) = \frac{1}{2}D_{tot}; D_1(0) = i\}$$
$$\text{with } i \in [\frac{1}{2}D_{tot}, D_{tot}],$$

and the hitting time τ_i of $D_1 = \frac{1}{2}D_{tot}$, starting from $D_1 = i$, as $\tau_i = \mathbb{E}(t_i)$. We want to calculate $\tau_{D_{tot}}$, which is the hitting time of state $D_1 = \frac{1}{2}D_{tot}$, starting from state $D_1 = D_{tot}$. Then, according to [13], we have

$$\begin{aligned}
&\tau_{\frac{1}{2}D_{tot}} = 0,\\
&\tau_x = \frac{1}{\alpha_x + \beta_x} + \frac{\beta_x}{\alpha_x + \beta_x}\tau_{x-1} + \frac{\alpha_x}{\alpha_x + \beta_x}\tau_{x+1}\\
&(\text{for } x = \frac{1}{2}D_{tot} + 1, \ldots, D_{tot} - 1),\\
&\tau_{D_{tot}} = \frac{1}{\beta_{D_{tot}}} + \tau_{D_{tot}-1},
\end{aligned} \tag{17}$$

where α_x and β_x are given in Fig. 2 (Fig. 1(a) column). By applying the same procedure from the previous subsection, we obtain

$$\begin{aligned}
\tau_{D_{tot}} &= \tau_{D_{tot}-1} + \frac{1}{\beta_{D_{tot}}}\\
&= (\tau_{D_{tot}-1} - \tau_{D_{tot}-2}) + \ldots + (\tau_1 - \tau_0) + \frac{1}{\beta_{D_{tot}}}\\
&= \sum_{x=\frac{1}{2}D_{tot}}^{D_{tot}-2} \Big(\sum_{j=x}^{D_{tot}-1} \frac{1}{\beta_j}\frac{\gamma_j}{\gamma_x} + \frac{1}{\beta_{D_{tot}}\gamma_x} \Big) + \frac{1}{\beta_{D_{tot}}}.
\end{aligned} \tag{18}$$

We next evaluate the expression of $\tau_{D_{tot}}$ given in (18) by substituting the specific expression of γ_x in Fig. 2 (Fig. 1(a) column).

Claim 4.3: The hitting time $\tau_{D_{tot}}$ satisfies $\tau_{D_{tot}} = \frac{\delta}{a\Delta I}(\frac{1}{4}D_{tot}^2 + \frac{1}{2}D_{tot} - 1)$ for system Fig. 1(a)

Proof: To calculate $\tau_{D_{tot}}$ for Fig. 1(a), we can obtain α_i and β_i from (4) as follows:

$$\alpha_0 = \ldots = \alpha_{D_{tot}-1} = \beta_1 = \ldots = \beta_{D_{tot}} = a\frac{\Delta I}{\delta} = \alpha,$$

which implies $\gamma_i = 1$. Then the hitting time $\tau_{D_{tot}}$ can be written as

$$\tau_{D_{tot}} = \sum_{x=\frac{1}{2}D_{tot}}^{D_{tot}-2} \Big(\sum_{D_{tot}-1}^{j=x} \frac{2}{\alpha} \Big) + \frac{1}{\alpha} = \frac{\delta}{a\Delta I}(\frac{1}{4}D_{tot}^2 + \frac{1}{2}D_{tot} - 1).$$

■

This claim shows that the hitting time $\tau_{D_{tot}}$ of the design in Fig. 1(a) is, just like for the design of Fig. 1(c), depends only on the leakiness, the protein's decay rate constant, and the recombinase switching rate constant, parameters that are not as easily tunable as a protein's expression rate c.

We therefore conclude that the design of Fig. 1(b) allows to extend the time to memory loss of either stable state by increasing the recombinases expression rate constants c_i, such as through increasing the RBS strength. By contrast, this is not possible in the other two designs, in which the effect of leakiness dictates the time to memory loss. This also implies that the presence of the intermediate state D in the design of Fig. 1(b) is critical to obtain a design where the degrading effect of leakiness on the time to memory loss can be quenched.

V. Simulation Result

Given that a number of approximations were made in order to achieve a system representation that could allow us to analytically write the hitting time as a function of the parameters, we perform simulations in this section to demonstrate that the trends discovered analytically hold in general for the original systems. Specifically, we use the Stochastic Simulation Algorithm (SSA) [11] to simulate the full systems of reactions given in (1), (5), (9), and, especially for system (5), without assuming time-scale separation between D and D_1, D_2.

Fig. 3 shows sample paths of D_1 for the three toggle switch designs for different ΔI and c values. D_1 starts from D_{tot} and longer memory implies that D_1 does not hit 0 (for designs in Fig. 1(b) and Fig.1(c)) or $\frac{1}{2}D_{tot}$ (for the design in Fig.1(a)) for longer time. As predicted from theory, the time to memory loss increases for all designs when the leakiness decreases (Fig. 3(a),(b),(d)). However, we cannot easily reduce the leakiness ΔI. By constrast, we can easily tune the expression rate constant c. As predicted from theory, the design of Fig. 1(b) shows increased time of memory loss when c is increased (Fig. 3(c)), while the design of Fig. 1(c) does not (Fig. 3(e)).

Fig. 4 further shows the numerically obtained stationary distribution of (D_1, D_2) for the three different toggle switch designs. Fig. 4(a)-(b) shows that the design of Fig. 1(a) has a unimodal stationary distribution, which is consistent with the fact that the circuit is monostable and not bistable, so it is not a good candidate to engineer memory. Fig. 4(c)-(e) and Fig.4(f)-(h) show that both designs in Fig. 1(b) and Fig. 1(c), which we have proposed, result in a bimodal distribution, consistent with bistability. However, only for the design in Fig. 1(b), but not for the design in Fig. 1(c), as c is increased the distribution becomes concentrated around the two deterministic stable steady states (Fig 4(e) versus Fig 4(h)). This is consistent with an increased time to memory loss since the probability of finding the system in any intermediate state becomes practically zero as c is increased.

VI. Conclusion

In this paper, we proposed a design for a long-term memory genetic toggle switch inspired by chromatin modification circuits. Our design overcomes the major drawback of conventional toggle switch designes based on DNA invertases, which are vulnerable to basal level of expression of the DNA invertases. We mathematically proved that the hitting time of state $D_1 = 0$ from state $D_1 = D_{tot}$ of our design can be increased, despite leakines, by increasing the invertases production rates. We also provided simulation results that

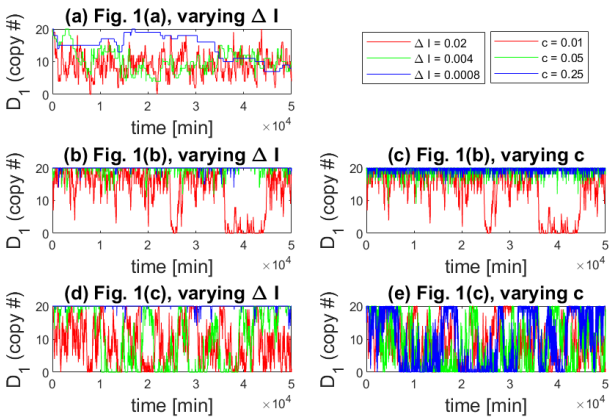

Fig. 3: **Time trajectories of D_1 for the three different toggles switch designs.** (a) Time trajectories of Fig. 1(a) with different ΔI (0.02, 0.004, 0.0008 mM min^{-1}). (b)-(c) Time trajectories of Fig. 1(b). For (b), c is fixed as 0.01 min^{-1} and ΔI is changed (0.02, 0.004, 0.0008 mM min^{-1}). For (c), ΔI is fixed as 0.02 min^{-1} and c is changed (0.01, 0.05, 0.25 min^{-1}). (d)-(e) Time trajectories of Fig. 1(c). For (d), c is fixed as 0.01 min^{-1} and ΔI is changed (0.02, 0.004, 0.0008 mM min^{-1}). For (e), ΔI is fixed as 0.02 min^{-1} and c is changed (0.01, 0.05, 0.25 min^{-1}). In all simulations, $a_1 = a_2 = a = b_1 = b_2 = 5.78 \times 10^{-3}$ mM^{-1}min^{-1}, $\delta_1 = \delta_2 = 0.069$ min^{-1}, $I_1 = I_2 = 0$ mM min^{-1}, $\Delta I_1 = \Delta I_2 = 0.02, 0.004, 0.0008$ mM min^{-1}, $D_{tot} = 20$, $c_1 = c_2 = c = 0.01, 0.05, 0.25$ min^{-1}, $(D_1(0), D_2(0)) = (D_{tot}, 0)$, time = 0 to 50000 minutes are used [12] [6]. For (b) and (c), since $a_1 = a_2 = b_1 = b_2$, the simulation is conducted outside the region of approximation of D to the quasi-steady state.

validate the theoretical predictions on the full reaction systems. More broadly, DNA invertases allow implementation of long-term memory bacterial toggle switches based on the core chromatin modification circuit motifs that shape epigenetic memory in eukaryotic cells.

References

[1] T. Ellis, X. Wang, and J. J. Collins, "Diversity-based, model-guided construction of synthetic gene networks with predicted functions," *Nature biotechnology*, vol. 27, no. 5, pp. 465–471, 2009.

[2] M. R. Atkinson, M. A. Savageau, J. T. Myers, and A. J. Ninfa, "Development of genetic circuitry exhibiting toggle switch or oscillatory behavior in escherichia coli," *Cell*, vol. 113, no. 5, pp. 597–607, 2003.

[3] H. Kobayashi, M. Kaern, M. Araki, K. Chung, T. S. Gardner, C. R. Cantor, and J. J. Collins, "Programmable cells: interfacing natural and engineered gene networks," *Proceedings of the National Academy of Sciences*, vol. 101, no. 22, pp. 8414–8419, 2004.

[4] J. W. Kotula, S. J. Kerns, L. A. Shaket, L. Siraj, J. J. Collins, J. C. Way, and P. A. Silver, "Programmable bacteria detect and record an environmental signal in the mammalian gut," *Proceedings of the National Academy of Sciences*, vol. 111, no. 13, pp. 4838–4843, 2014.

[5] W. Bothfeld, G. Kapov, and K. E. Tyo, "A glucose-sensing toggle switch for autonomous, high productivity genetic control," *ACS synthetic biology*, vol. 6, no. 7, pp. 1296–1304, 2017.

[6] J. Fernandez-Rodriguez, L. Yang, T. E. Gorochowski, D. B. Gordon, and C. A. Voigt, "Memory and combinatorial logic based on dna inversions: dynamics and evolutionary stability," *ACS synthetic biology*, vol. 4, no. 12, pp. 1361–1372, 2015.

[7] T. S. Moon, E. J. Clarke, E. S. Groban, A. Tamsir, R. M. Clark, M. Eames, T. Kortemme, and C. A. Voigt, "Construction of a genetic multiplexer to toggle between chemosensory pathways in escherichia coli," *Journal of molecular biology*, vol. 406, no. 2, pp. 215–227, 2011.

[8] I. B. Dodd, M. A. Micheelsen, K. Sneppen, and G. Thon, "Theoretical analysis of epigenetic cell memory by nucleosome modification," *Cell*, vol. 129, no. 4, pp. 813–822, 2007.

[9] S. Bruno, R. J. Williams, and D. Del Vecchio, "Epigenetic cell memory: The gene's inner chromatin modification circuit," *PLoS computational biology*, 2022.

[10] P. Klemm, "Two regulatory fim genes, fimb and fime, control the phase variation of type 1 fimbriae in escherichia coli.," *The EMBO journal*, vol. 5, no. 6, pp. 1389–1393, 1986.

[11] D. Del Vecchio and R. M. Murray, *Biomolecular feedback systems*. Princeton University Press, 2014.

[12] Y. Qian, H.-H. Huang, J. I. Jiménez, and D. Del Vecchio, "Resource competition shapes the response of genetic circuits," *ACS synthetic biology*, vol. 6, no. 7, pp. 1263–1272, 2017.

[13] J. R. Norris, *Markov chains*. No. 2, Cambridge university press, 1998.

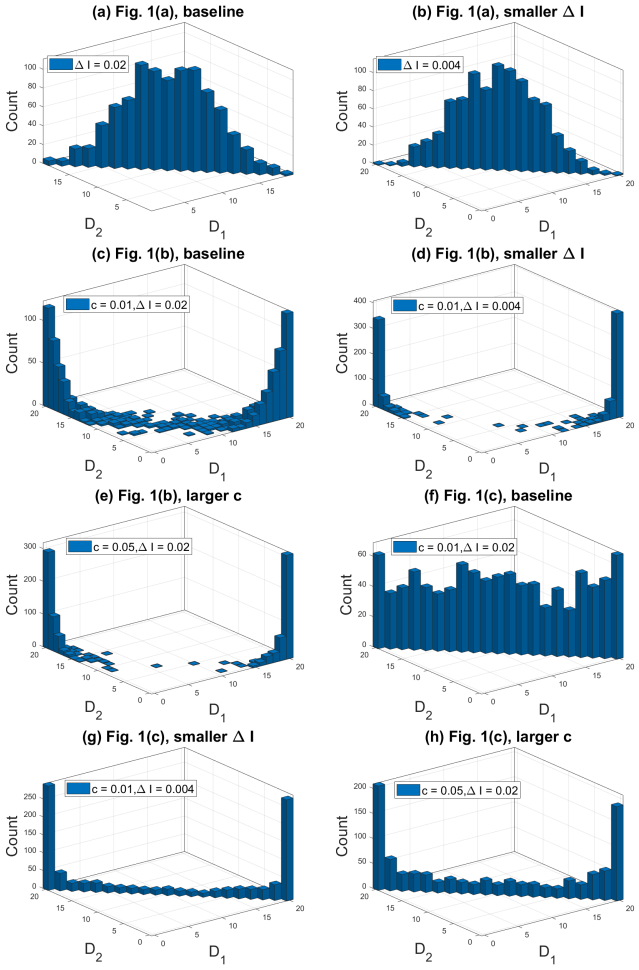

Fig. 4: **Stationary distribution of (D_1, D_2) for the three different toggle switch designs.** (a)-(b) Stationary distribution of the system in Fig. 1(a) for different ΔI ((a): $\Delta I = 0.02$ mM min^{-1}, (b): $\Delta I = 0.004$ mM min^{-1}). (c)-(e) Stationary distribution of the system in Fig. 1(b) for different c and ΔI ((c): $c = 0.01$ min^{-1}, $\Delta I = 0.02$ mM min^{-1}, (d): $c = 0.01$ min^{-1}, $\Delta I = 0.004$ min^{-1}, (e): $c = 0.05$ min^{-1}, $\Delta I = 0.02$ mM min^{-1}) (f)-(h) Stationary distribution of the system in Fig.1(c) for different c and ΔI ((f): $c = 0.01$ min^{-1}, $\Delta I = 0.02$ mM min^{-1}, (g): $c = 0.01$ min^{-1}, $\Delta I = 0.004$ mM min^{-1}, (h): $c = 0.05$ min^{-1}, $\Delta I = 0.02$ mM min^{-1}). All parameters are the same as those in Fig. 3. Stationary distributions were obtained by simulating the system for 1000 different initial conditions and for $t_f = 200000$ min.